

# Systematic Analysis of Smooth Muscle and Cartilage Ring Formation during Mouse Tracheal Tubulogenesis

Haoyu Wu<sup>1,2,#</sup>, Ping Wang<sup>3,#</sup>, Ziying Liu<sup>1</sup>, Chunyan Lu<sup>1</sup>, and Wenguang Yin<sup>1,2,4,5,6,\*</sup>

<sup>1</sup>State Key Laboratory of Respiratory Disease, National Clinical Research Center for Respiratory Disease, Guangzhou Institute of Respiratory Health, the First Affiliated Hospital of Guangzhou Medical University, GMU-GIBH Joint School of Life Sciences, Guangzhou Medical University, Guangzhou Medical University, Guangzhou, Guangdong, China

<sup>2</sup>Guangzhou National Laboratory, No. 9 XingDaoHuanBei Road, Guangzhou International Bio Island, Guangzhou, Guangdong Province, China

<sup>3</sup>Guangzhou Women and Children's Medical Center, Guangzhou, Guangdong, China

<sup>4</sup>GMU-GIBH Joint School of Life Sciences, Guangzhou Medical University, Guangzhou, Guangdong, China

<sup>5</sup>Key Laboratory of Biological Targeting Diagnosis, Therapy and Rehabilitation of Guangdong Higher Education Institutes, the Fifth Affiliated Hospital of Guangzhou Medical University, Guangzhou, Guangdong, China

<sup>6</sup>Max Planck Institute for Heart and Lung Research, Department of Developmental Genetics, Bad Nauheim, Germany

\*For correspondence: [yin\\_wenguang@gzhmu.edu.cn](mailto:yin_wenguang@gzhmu.edu.cn)

#Contributed equally to this work

## Abstract

The trachea tube is the exclusive route to allow gas exchange between the external environment and the lungs. Recent studies have shown the critical role of mesenchymal cells in tracheal tubulogenesis. Improved methods for studying the dynamics of the tracheal mesenchyme development are needed to investigate the cellular and molecular mechanisms during tracheal tubulogenesis. Here, we describe a detailed protocol for a systematic analysis of tracheal tube development to enable observing tracheal smooth muscle (SM) and cartilage ring formation. We describe immunostaining, confocal and stereomicroscopy imaging, and quantitative methods to study the process of tracheal SM and cartilage ring development, including SM cell alignment, polarization, and changes in cell shape as well as mesenchymal condensation. The technologies and approaches described here not only improve analysis of the patterning of the developing trachea but also help uncover the mechanisms underlying airway disease. This protocol also provides a useful technique to analyze cell organization, polarity, and nuclear shape in other organ systems.

**Keywords:** Trachea, Smooth muscle cell, Cartilage, Mesenchymal condensation, Cell polarity

**This protocol is used in:** Nat. Commun. (2018), DOI: 10.1038/s41467-018-05043-5; Eur. Respir J. (2019), DOI:10.1183/13993003.00840-2018

## Background

Understanding tracheal formation is a fundamental goal in the field of pulmonary development and disease. The trachea consists of mesoderm-derived smooth muscle (SM), cartilage, and connective tissue, as well as endoderm-derived epithelium (Brand-Saberi and Schafer, 2014). SM is positioned dorsally to control tracheal contraction, whereas the cartilage rings are located ventrally to prevent airway collapse (Hines et al., 2013; Yin et al., 2018 and 2019).

In humans, defects in the formation of the tracheal tube have been reported to lead to tracheomalacia, tracheostenosis, or complete tracheal ring deformity, which are characterized by a deficiency of the supporting cartilage or narrowing of the tracheal lumen and may lead to respiratory distress and death (Landing and Dixon, 1979; Fraga et al., 2016; Sinner et al., 2019).

In mice, tracheal SM differentiation starts by embryonic day 11.5 (E11.5) with the appearance of  $\alpha$ -smooth muscle actin ( $\alpha$ SMA) positive cells at the dorsal side (Hines et al., 2013; Yin et al., 2018). Newly differentiated tracheal SM cells exhibit round shapes and are not well organized (Yin et al., 2018 and 2019). They progressively develop into spindle-shaped cells that circumferentially align the tube (Yin et al., 2018 and 2019). During tracheal elongation, differentiated SM cells proliferate with increased area of SM stripes from E11.5 to P0 (Yin et al., 2018).

Tracheal cartilage development initiates as early as E9 (Elluru and Whitsett, 2004). Uncondensed SOX9<sup>+</sup> mesenchymal cells appear and are restricted to the ventral trachea as early as E10.5 (Hines et al., 2013). Both *Sox9* mRNA levels and the number of SOX9<sup>+</sup> mesenchymal cells increase at E12.5 (Hines et al., 2013). By E13.5, SOX9<sup>+</sup> mesenchymal cells condense to resemble cartilaginous rings with the number of 11–13. The number of C-shaped rings appears to be unchanged, whereas both the distance between rings and ring width increase during tracheal elongation (Yin et al., 2019). By E15.5, SOX9<sup>+</sup> mesenchymal cells start differentiating into chondrocytes characterized by positive alcian blue staining, as well as aggrecan and type II collagen expression (Park et al., 2010; Yin et al., 2019).

Analysis of tracheal formation has mostly focused on cell condensation, differentiation, proliferation, and apoptosis by using tissue sections (Park et al., 2010; Hines et al., 2013; Lin et al., 2014). These studies have provided information on cell behavior in two-dimensional views, allowing for a better understanding of the cellular and molecular mechanisms underlying tracheal tubulogenesis. The method we present here for whole-mount immunostaining and imaging overcomes some of their limitations; for example, the precise sites of the three-dimensional trachea are not properly located. Thus, it is presently unclear how cells are organized in the whole trachea. Another not fully investigated question is the characteristics of SM cells. Although SM cell differentiation and proliferation have been tested (Hines et al., 2013; Gerhardt et al., 2018), cell alignment, polarization, and changes in cell shape in tracheal development remain largely unknown. To analyze tissue structure and cell organization, we provide a detailed protocol for examining SM cell organization and changes in cell shape as well as mesenchymal cell condensation, an important process during tracheal cartilage formation (Yin et al., 2019).

## Materials and reagents

1. Coverslips (Thermo Fisher Scientific, catalog number: 11961988)
2. Adhesion slides (Thermo Fisher Scientific, catalog number: 10219280)
3. 10 cm Petri dish (Corning, catalog number: 430167)
4. Pipette (Sigma-Aldrich, catalog number: Z331759-1PAK)
5. Cy3-conjugated anti-mouse  $\alpha$ SMA (Sigma-Aldrich, catalog number: C6198)
6. Anti-rat CDH1 (E-cadherin) (Santa Cruz, catalog number: sc-59778)
7. Anti-rabbit SOX9 (SRY-box transcription factor 9) (Millipore, catalog number: AB5535)
8. Sheep anti-GM130/GOLGA2 (Golgin subfamily A member 2) (R&D systems, catalog number: AF8199)
9. Paraformaldehyde (PFA) (Sigma-Aldrich, catalog number: 30525-89-4)
10. Dimethyl sulfoxide (DMSO) (Sigma-Aldrich, catalog number: D8418)
11. Mowiol (Millipore, catalog number: 475904)
12. 30% hydrogen peroxide (H<sub>2</sub>O<sub>2</sub>) (Sigma-Aldrich, catalog number: 7722-84-1)

13. Methanol (Sigma-Aldrich, catalog number: 34860)
14. Bovine serum albumin (BSA) (Thermo Fisher Scientific, catalog number: 30036578)
15. Fetal bovine serum (FBS) (Gibco, catalog number: 10270-106)
16. 4',6-Diamidino-2-Phenylindole, dilactate (DAPI) (Thermo Fisher Scientific, catalog number: D3571)
17. Phosphate buffered saline (PBS) (Capricorn Scientific, catalog number: PBS-1A)
18. Hanks' balanced salt solution (HBSS) (Sigma-Aldrich, catalog number: H6648)
19. Triton X-100 (Sigma-Aldrich, catalog number: 9036-19-5)
20. Glycerol (Sigma-Aldrich, catalog number: USA56-81-5)
21. Benzyl benzoate (Sigma-Aldrich, catalog number: B6630)
22. Benzyl alcohol (Sigma-Aldrich, catalog number: 305197)
23. Benzyl benzoate (Sigma-Aldrich, catalog number: B6630-1L)
24. Sucrose (Sigma-Aldrich, catalog number: 57-50-1)
25. Tissue-Tek OCT (SAKURA, catalog number: 4583)
26. Goat anti-rabbit IgG (H+L) highly cross-adsorbed secondary antibody, Alexa Fluor™ 488 (Thermo Fisher Scientific, catalog number: A-11034)
27. Donkey anti-sheep IgG (H+L) secondary antibody, Alexa Fluor™ 647 (Thermo Fisher Scientific, catalog number: A-21448)
28. Goat anti-rat IgG (H+L) secondary antibody, Alexa Fluor™ 568 (Thermo Fisher Scientific, catalog number: A-11077)
29. Phosphate buffered saline (PBS) (see Recipes)
30. 4% formaldehyde solution (see Recipes)
31. Permeabilization solution (see Recipes)
32. 10% sucrose (see Recipes)
33. 30% sucrose (see Recipes)
34. Mowiol mounting medium (see Recipes)
35. 0.3% Triton X-100/PBS solution (see Recipes)
36. 5% FBS/PBS/0.5% Triton X-100/3% BSA solution (see Recipes)
37. 70% ethanol solution (see Recipes)
38. DMSO:methanol (1:4) solution (see Recipes)
39. H<sub>2</sub>O<sub>2</sub>/DMSO/methanol (1:1:4) solution (see Recipes)
40. 80% methanol solution (see Recipes)
41. 50% methanol solution (see Recipes)
42. Benzyl alcohol:benzyl benzoate (BABB) (1:2) solution (see Recipes)
43. 5% FBS/PBS/3% BSA blocking solution (see Recipes)

## Equipment

1. Scissors (FST, catalog number: 15011-12)
2. Forceps (FST, catalog number: 11252-20)
3. Stereoscopic dissecting microscope (Zeiss, model: Stemi 305)
4. Stereomicroscope (Nikon, model: SMZ25)
5. Upright laser scanning confocal microscope (Zeiss, model: LSM 880) or cryostat (Leica, model: CM1950)
6. Quantification of immunofluorescence intensity of lumen area, tube length, SM area, SM cell orientation, nuclear, aspect ratio (NAR), and Golgi-apparatus position relative to the nucleus was performed using ImageJ (Version 1.8.0.172) (Schneider et al., 2012)

## Software

1. ImageJ, GraphPad Prism (Version 8.0.2)

2. Zeiss ZEN (Version 2.3)

## Procedure

A schematic diagram of the protocol overview is presented in Figure 1.

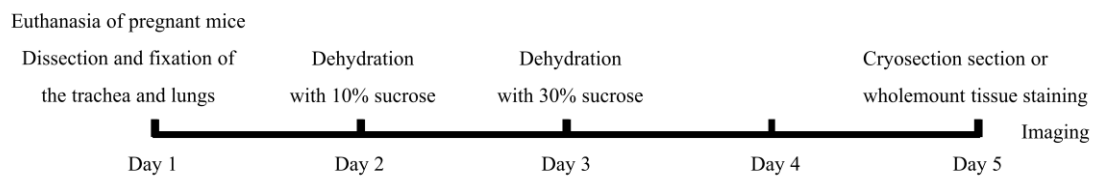


**Figure 1. Schematic diagram of the protocol overview**

### A. Mouse tracheal dissection

1. Euthanize pregnant mice at E11.5–E16.5 by CO<sub>2</sub> exposure, consistent with institutional ethical guidelines and approved protocols. Place one mouse in a CO<sub>2</sub> chamber and gradually fill CO<sub>2</sub> at a flow rate of 20% of the chamber volume per minute. Keep the animal in the chamber for 4 min and maintain gas flow for an additional 2 min after apparent clinical death. Perform cervical dislocation following CO<sub>2</sub> treatment (Figure 1).
2. Isolate embryos from euthanized animals. Clean and sterilize the abdomen with 70% ethanol. Perform laparotomy using surgical scissors and forceps. Transfer the uterus and keep it in ice-cold HBSS in a 10 cm Petri dish. Open the uterus and transfer embryos to a new dish containing ice-cold HBSS (Supplementary Figure 1).
3. Dissect the trachea and lungs from the embryo under the stereoscopic dissecting microscope. For embryonic mice, it is best to start dissection from the abdominal cavity so as not to damage the trachea and lungs in the thoracic cavity. Fix the head and forelimb, remove the skin, carefully open the abdominal cavity not to damage the trachea and lungs, and remove the heart using scissors and forceps. Separate the trachea and lungs from the embryo and trim away the esophagus using forceps. The trachea is cut above the larynx to ensure its integrity. The esophagus is dissected behind the trachea and down from the larynx with two tiny forceps. Transfer the trachea and lungs to a 24-well plate containing ice-cold PBS using a 1 mL pipette to ensure tissue integrity (Supplementary Figure 1 and Supplementary Figure 2).

### B. Whole-mount immunostaining and imaging

1. The mouse embryonic trachea is tiny. To avoid sucking it away in washing procedures, we perform whole-mount immunostaining using the whole trachea and lungs and suck out washing buffer when tissues sink to the bottom of the tube. Fix E11.5–E16.5 tracheas and lungs in DMSO:methanol (1:4) (see Recipes) overnight at 4 °C. Incubate samples in H<sub>2</sub>O<sub>2</sub>/DMSO/methanol (1:1:4) (see Recipes) for 5 h at room temperature (RT). The purpose of soaking the tissue in a fixative containing hydrogen peroxide is to remove endogenous catalase.
2. Wash samples twice in 100% methanol for 1 h each, once in 80% methanol for 1 h, once in 50% methanol for 1 h, twice in PBS for 1 h each, and twice in 5% FBS/PBS/0.5% Triton X-100/3% BSA (see Recipes) for 1 h each.
3. Incubate tracheas and lungs in primary antibodies diluted in 5% FBS/PBS/0.5% Triton X-100/3% BSA (SOX9, 1:400; αSMA-Cy3, 1:200; GM130, 1:50) for 24 h at 4 °C. Wash samples five times in 5% FBS/PBS/0.5% Triton X-100/3% BSA for 1 h each at 4 °C.

4. Incubate samples in secondary antibodies (Alexa Fluor 488, 1:1,000; Alexa Fluor 647, 1:1,000; DAPI, 1:2,000) for 24 h at 4 °C. Wash samples five times in 5% FBS/PBS/0.5% Triton X-100/3% BSA for 1 h each at 4 °C.
5. Dehydrate samples in methanol for 6 h (incomplete dehydration may result in tissue disintegration), and then clear samples in BABB (1:2) (see Recipes) for 24 h.
6. Mount samples in BABB and seal the edges of the cover glass completely with nail polish.
7. After whole-mount immunostaining, tissues are transferred to the microscope for imaging. The position of the trachea is gently adjusted with a pipette as follows: throat and upper trachea in the anterior direction, lower trachea in the posterior direction, cartilage in the upward direction, and SM in the downward direction to obtain a dorsal and ventral view. Acquire images of tracheal SM and cartilage rings in an anterior–posterior direction with a laser scanning confocal microscope by using a 20× objective and a stereomicroscope with a fluorescence mode by using a 2.5× objective, respectively. Take 10–15 images for whole-mount immunostaining. Take one image for section immunostaining (Figure 1; Figure 2A, 2C, 2E, 2G; Figure 5A–5D).

### C. Immunostaining of sections and imaging

1. Fix E11.5–E14.5 tracheas and lungs in 4% PFA overnight at 4 °C. Incubate samples in 10% and 30% sucrose for 24 h each at 4 °C.
2. Mount samples in OCT embedding compound. Make transverse sections of the trachea at 10 μm.
3. Fix sections in 4% PFA for 10 min at 4 °C. Incubate samples in permeabilization solution (0.25% Triton X-100/PBS) (see Recipes) for 15 min at RT and in blocking solution (5% FBS/PBS/3% BSA) for 1 h at RT.
4. Incubate samples in primary antibodies (αSMA-Cy3, 1:1,000; CDH1, 1:200, or SOX9, 1:400) overnight at 4 °C. Wash samples three times in 5% FBS/PBS/0.5% Triton X-100/3% BSA for 10 min each at RT.
5. Incubate samples in secondary antibodies [Alexa Fluor™ 568 goat anti-rat IgG (H+L), 1:1,000 or Alexa Fluor™ 488 goat anti-rabbit IgG (H+L), 1:1,000] for 2 h at RT. Wash samples three times in 5% FBS/PBS/0.5% Triton X-100/3% BSA for 10 min each at RT.
6. Perform DAPI counterstaining (1:2,000) for 5 min at RT. Wash samples three times in 5% FBS/PBS/0.5% Triton X-100/3% BSA for 10 min each at RT.
7. Mount samples with Mowiol mounting medium. Acquire images using a laser scanning confocal microscope (Figure 1; Figure 4A, 4C, 4E, and Figure 5E).

### D. Quantification of SM cell alignment

1. Select the whole area of the imaged tracheal SM.
2. Draw a horizontal line and then a line along the extension of a SM cell using the angle tool in ImageJ. Select the menu Analyze and click the button Measure. Record the value of the angle for each SM cell.
3. For an individual trachea, measure the value of the angle for 50 SM cells. Quantify six tracheas. Count the number of SM cells in each defined angle value range (-90° to -30°, -30° to 0°, 0° to 30°, 30° to 90°). Calculate the ratio of SM cells (Figure 2).

*Note: Distribution of SM cell alignment is reflected by the percentage of SM cells in the defined angle value range.*

### E. Quantification of SM cell polarity

1. Select the whole area of the imaged tracheal SM.
2. The Golgi apparatus for polarity analysis has been used in airway SM cells and vascular endothelial cells (Kwon et al., 2016; Yin et al., 2018). Draw a horizontal line to the middle of the SM cell nucleus and then a line to the GM130-labeled Golgi using the angle tool in ImageJ. Select the menu Analyze and click the button Measure. Record the value of angle for each SM cell.

- For an individual trachea, measure the value of the angle for 50 SM cells. Quantify six tracheas. Count the number of SM cells in each defined angle value range (-135° to -45°, -45° to 45°, 45° to 135°, 135° to -135°) (Chen et al., 2015). Calculate the ratio of SM cells (Figure 3).

*Note: Distribution of SM cell polarity is reflected by the percentage of SM cells in the defined angle value range.*

## F. Quantification of SM cell nuclear aspect ratio (NAR)

- Select the whole area of the imaged tracheal SM.
- Draw a line along the horizontal dimension of the SM cell nucleus using Straight Line in ImageJ and assign it as the length  $2a$ . Select the menu Analyze and click the button Measure. Record the value of length (Supplementary Figure 3).
- Draw a line perpendicularly across the middle of the length using Straight Line in ImageJ and assign it as the width  $2b$ . Select the menu Analyze and click the button Measure. Record the value of length (Supplementary Figure 3).
- Calculate the value of NAR using the equation:  

$$\text{NAR} = a/b$$
- For an individual trachea, calculate the value of NAR for 50 SM cells. Quantify six tracheas. Count the number of SM cells in each defined NAR range (0–1.0, 1.0–2.0, 2.0–3.0, 3.0–4.0). Calculate the ratio of SM cells.

*Note: Distribution of SM cell shape is reflected by the percentage of SM cells in the defined NAR value range.*

## Data analysis

### Results

#### SM cell alignment

SM is critical for tubulogenesis in the trachea, lungs, gut, and blood vessels (Knot and Nelson, 1998; Shyer et al., 2013; Kim et al., 2015; Yin et al., 2018 and 2019). To analyze SM organization during tracheal formation, we examined SM cell alignment using  $\alpha$ SMA antibody staining. SM cells were aligned approximately perpendicular to the direction of tube elongation from E12.5 to P60 (Figure 2A–2H). SM exhibited no significant differences in cell alignment among these stages.

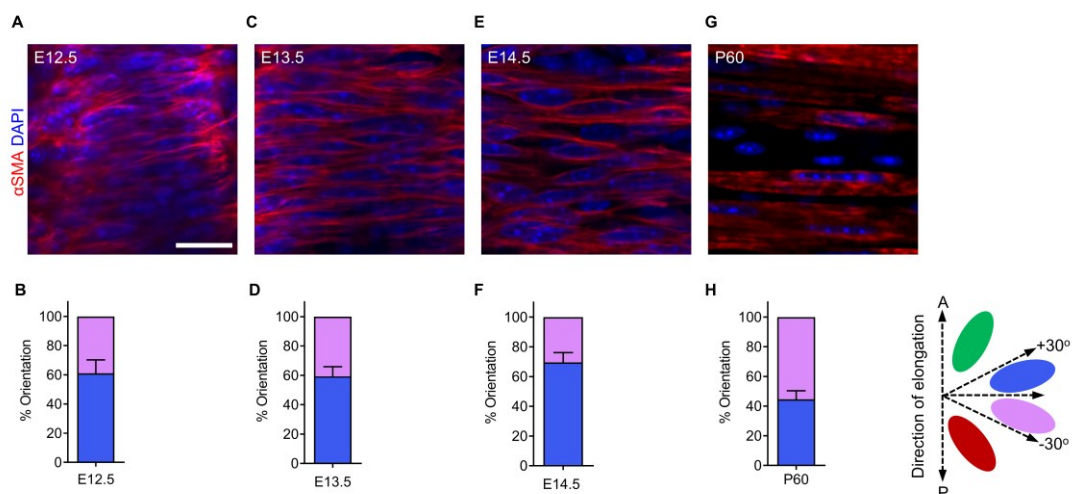


**Figure 2. Tracheal smooth muscle (SM) cell alignment at several embryonic and postnatal stages. (A) Dorsal**

views of  $\alpha$ SMA immunostaining (red) and DAPI staining (blue) of E12.5 tracheas. (B) Quantification of E12.5 tracheal SM cell orientation ( $n = 7$ ). (C) Dorsal views of  $\alpha$ SMA immunostaining (red) and DAPI staining (blue) of E13.5 tracheas. (D) Quantification of E13.5 tracheal SM cell orientation ( $n = 7$ ). (E) Dorsal views of  $\alpha$ SMA immunostaining (red) and DAPI staining (blue) of E14.5 tracheas. (F) Quantification of E14.5 tracheal SM cell orientation ( $n = 7$ ). (G) Dorsal views of  $\alpha$ SMA immunostaining (red) and DAPI staining (blue) of P60 tracheas. (H) Quantification of P60 tracheal SM cell orientation ( $n = 7$ ). Scale bar = 20  $\mu$ m (A, C, E, G).

### SM cell polarity

Correct orientation of the cell body depends on the establishment of cell polarity (Li and Dudley, 2009). To examine the polarization of tracheal SM cells, we quantified the Golgi apparatus position relative to the nucleus by using the *cis*-Golgi matrix marker GM130 (Nobes and Hall, 1999; Kwon et al., 2016). GM130<sup>+</sup> Golgi localized preferentially along the longitudinal edges of the nucleus in SM cells at E14.5 (Figure 3A and 3B).



**Figure 3. Tracheal smooth muscle (SM) cell polarity at E14.5.** (A) Immunostaining for  $\alpha$ SMA (red) and GM130 (green) and DAPI staining (blue) in dorsal views of E14.5 tracheas. (B) Quantification of E14.5 Golgi apparatus (green) position relative to the nucleus (blue) ( $n = 8$ ). Scale bar = 20  $\mu$ m (A and B).

### SM cell NAR

To examine changes in SM cell shape during tracheal formation, we examined NAR. SM cells exhibited approximately round shapes at E11.5–E12.5 (Figure 4A–4D) and developed spindle shapes by E13.5 (Figure 4E and 4F), indicating that SM cell elongates significantly between E12.5 and E13.5.

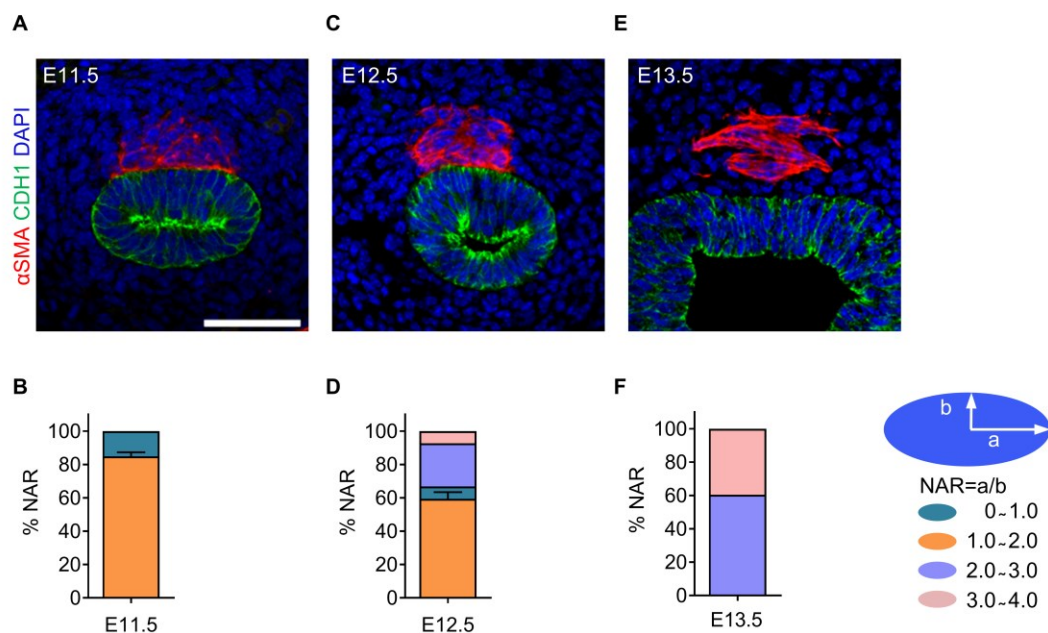


**Figure 4. Tracheal smooth muscle (SM) cell nuclear aspect ratio (NAR) at several embryonic stages.** (A) Immunostaining for  $\alpha$ SMA (red) and CDH1 (green), and DAPI staining (blue) of transverse sections of E11.5

tracheas. (B) Quantification of E11.5 tracheal SM cell NAR (n = 6). (C) Immunostaining for  $\alpha$ SMA (red) and CDH1 (green), and DAPI staining (blue) of transverse sections of E12.5 tracheas. (D) Quantification of E12.5 tracheal SM cell NAR (n = 6). (E) Immunostaining for  $\alpha$ SMA (red) and CDH1 (green), and DAPI staining (blue) of transverse sections of E13.5 tracheas. (F) Quantification of E13.5 tracheal SM cell NAR (n = 6). Scale bar = 20  $\mu$ m (A, C, E).

### Mesenchymal condensation

The condensation of mesenchymal cells into chondrogenic nodules drives chondrogenesis (Bi et al., 1999; Sala et al., 2011). To analyze the process of tracheal cartilage ring formation, we examined mesenchymal condensation in E12.5–E16.5 tracheas by using SOX9 antibody staining. An even distribution of SOX9<sup>+</sup> mesenchymal cells was observed in E12.5 tracheas (Figure 5A). Starting at E13.5, a clear pattern of condensed SOX9<sup>+</sup> mesenchymal cells resembling C-shaped cartilaginous rings was readily distinguished (Figure 5B), and these rings are becoming clearer at E14.5 and E16.5 (Figure 5C–5E), indicating that mesenchymal condensation begins between E12.5 and E13.5.

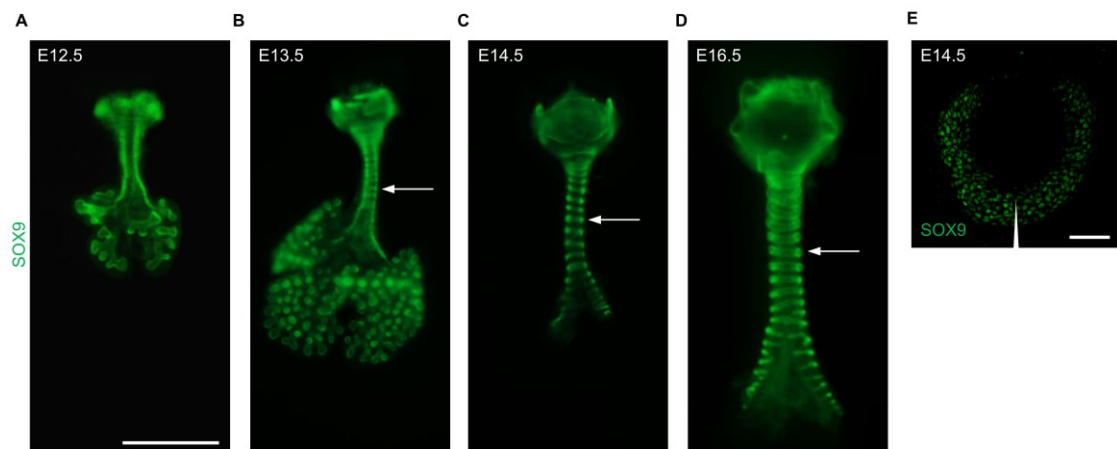


**Figure 5. Tracheal mesenchymal condensation at several embryonic stages.** (A) Immunostaining for SOX9 (green) in ventral views of E12.5 tracheas. (B) Immunostaining for SOX9 (green) in ventral views of E13.5 tracheas. (C) Immunostaining for SOX9 (green) in ventral views of E14.5 tracheas. (D) Immunostaining for SOX9 (green) in ventral views of E16.5 tracheas. (E) Immunostaining for SOX9 of transverse sections of E14.5 tracheas. Arrows point to tracheal rings. The arrowhead points to the ventral part of the trachea. Scale bar = 1 mm (A–D); 50  $\mu$ m (E).

### Discussion

In this protocol, we provided detailed descriptions about tissue preparation, immunostaining, clearing, and imaging as well as novel methods to measure tracheal SM cell alignment, polarity, and NAR. By using immunostaining in both whole-mount and sectioned tracheas at several embryonic stages in combination with confocal and stereomicroscopy imaging, we clearly observed the process of tracheal SM cell organization and changes in cell shape as well as mesenchymal condensation. Our methods enable researchers to visualize and analyze how tracheal mesenchyme forms and identify key timepoint(s) for cell behavior, organization, and shape changes (Hines et al., 2013; Lin et al., 2014; Park et al., 2010).

It is necessary to use the intact trachea for whole-mount immunostaining and quantification of SM cells and cartilage rings. Isolation of the tracheas from early embryos is not easy due to its fragility and tight connection with surrounding tissues. We used fine forceps to carefully remove tissues surrounding the trachea under stereomicroscopy.

SM lies beneath other mesenchymal cells in the dorsal part of the trachea. For fluorescence imaging of SM cells in the whole-mount immunostained trachea, it is critical to clear samples. We used BABB to transparentize the trachea to make deep structures visible without compromising immunofluorescence.

A limitation of this protocol is that fixation of the trachea will disable live-cell imaging. To track live cell behavior, we need to generate mouse lines expressing fluorescent reporters in mesenchymal cells such as *SOX9*<sup>CreERT2/+</sup>;*ROSA*<sup>mT/mG</sup> or *Myh11*<sup>CreERT2/+</sup>;*ROSA*<sup>mT/mG</sup> mice (same as *SMMHC*<sup>CreERT2/+</sup>;*ROSA*<sup>mT/mG</sup> mice)



(Muzumdar et al., 2007; Wirth et al., 2008; Soeda et al., 2010), and perform time-lapse imaging. SM cells surround epithelial and endothelial tubes in a number of organ systems, including the digestive tract, exocrine glands, lungs, kidneys, and vasculature (Hogan and Kolodziej, 2002; Iruela-Arispe and Beitel, 2013). Our protocol provides a useful technique to analyze SM cell organization, polarity, and nuclear shape in these organs.

## Recipes

### 1. Phosphate-buffered saline (PBS)

8.0 g of NaCl  
 0.2 g of KCl  
 1.15 g of Na<sub>2</sub>HPO<sub>4</sub>·7H<sub>2</sub>O  
 0.2 g of KH<sub>2</sub>PO<sub>4</sub>  
 Adjust to pH 7.4

### 2. 4% formaldehyde solution

40 g of PFA powder  
 Add 1× PBS up to 1 L

### 3. Permeabilization solution

1× PBS containing 0.25% Triton X-100

### 4. 10% sucrose

5 g of sucrose  
 Add distilled deionized water up to 50 mL per tube

### 5. 30% sucrose

15 g of sucrose  
 Add distilled deionized water up to 50 mL per tube

### 6. Mowiol mounting medium

200 mL of 1× PBS  
 50 g of Mowiol  
 25 mL of water-free glycerol  
 Add 50 g of Mowiol to 20 mL of 1× PBS, stir for 16 h at RT, add 25 mL of water-free glycerol, stir for 16 h at RT, centrifuge at 1,3525× g for 15 min at 4 °C, and store at -20 °C before use.

### 7. 0.3% Triton X-100/PBS solution

0.3 mL of Triton X-100  
 Add 1× PBS up to 1 L

### 8. 5% FBS/PBS/0.5% Triton X-100/3% BSA solution

50 mL of FBS  
 0.5 mL of Triton X-100  
 30 g of BSA  
 949.5 mL of 1× PBS

### 9. 70% ethanol solution

737 mL of 95% ethanol  
 Add distilled deionized water up to 1 L

**10. DMSO:methanol (1:4) solution**

50 mL of DMSO  
200 mL of methanol

**11. H<sub>2</sub>O<sub>2</sub>/DMSO/methanol (1:1:4) solution**

100 mL of 30% H<sub>2</sub>O<sub>2</sub>  
100 mL of DMSO  
400 mL of methanol

**12. 80% methanol solution**

Diluting 400 mL of methanol  
Add distilled deionized water up to 500 mL

**13. 50% methanol solution**

Diluting 250 mL of methanol  
Add distilled deionized water up to 500 mL

**14. Benzyl alcohol:benzyl benzoate (BABB) (1:2) solution**

50 mL of benzyl alcohol  
100 mL of benzyl benzoate

**15. 5% FBS/PBS/3% BSA blocking solution**

50 mL of FBS  
30 g of BSA  
950 mL of 1× PBS

## Acknowledgments

The author would like to acknowledge State Key Laboratory of Respiratory Disease, Guangzhou, Max Planck Institute for Heart and Lung Research, Bad Nauheim for the assistance and previous work (Yin et al., 2018 and 2019). This work was supported by the National Natural Science Foundation of China (81970019) and R&D Program of Guangzhou Laboratory (SRPG22-016 and SRPG22-021). Open Project of the State Key Laboratory of Respiratory Disease (SKLRD-OP-202110). Open Research Fund of State Key Laboratory of Genetic Engineering, Fudan University (No. SKLGE-2305).

## Competing interests

The author has nothing to disclose.

## Ethical considerations

C57BL/6J mice were used in the experiments. All mouse husbandry was performed under standard conditions in accordance with the Institutional Animal Care and Use Committees of Guangzhou Medical University, and institutional (Max Planck Society) and local ethics committee (Regierungspräsidium Darmstadt, Hessen, Germany). All animal experiments were performed in compliance with ethical guidelines and approved protocols.

## References

- Bi, W., Deng, J. M., Zhang, Z., Behringer, R. R. and de Crombrughe, B. (1999). [Sox9 is required for cartilage formation](#). *Nat Genet* 22(1): 85-89.
- Brand-Saberi, B. E. M. and Schafer, T. (2014). [Trachea: anatomy and physiology](#). *Thorac Surg Clin* 24(1): 1-5
- Chen, B., Co, C. and Ho, C. C. (2015). [Cell shape dependent regulation of nuclear morphology](#). *Biomaterials* 67: 129-136.
- Elluru, R. G. and Whitsett, J. A. (2004). [Potential role of Sox9 in patterning tracheal cartilage ring formation in an embryonic mouse model](#). *Arch Otolaryngol Head Neck Surg* 130(6): 732-736.
- Fraga, J. C., Jennings, R. W. and Kim, P. C. (2016). [Pediatric tracheomalacia](#). *Semin Pediatr Surg* 25(3): 156-164.
- Gerhardt, B., Leesman, L., Burra, K., Snowball, J., Rosenzweig, R., Guzman, N., Ambalavanan, M. and Sinner, D. (2018). [Notum attenuates Wnt/beta-catenin signaling to promote tracheal cartilage patterning](#). *Dev Biol* 436(1): 14-27.
- Hines, E. A., Jones, M. K., Verheyden, J. M., Harvey, J. F. and Sun, X. (2013). [Establishment of smooth muscle and cartilage juxtaposition in the developing mouse upper airways](#). *Proc Natl Acad Sci U S A* 110(48): 19444-19449.
- Hogan, B. L. and Kolodziej, P. A. (2002). [Organogenesis: molecular mechanisms of tubulogenesis](#). *Nat Rev Genet* 3(7): 513-523.
- Iruela-Arispe, M. L. and Beitel, G. J. (2013). [Tubulogenesis](#). *Development* 140(14): 2851-2855.
- Kim, H. Y., Pang, M. F., Varner, V. D., Kojima, L., Miller, E., Radisky, D. C. and Nelson, C. M. (2015). [Localized Smooth Muscle Differentiation Is Essential for Epithelial Bifurcation during Branching Morphogenesis of the Mammalian Lung](#). *Dev Cell* 34(6): 719-726.
- Kishimoto, K., Tamura, M., Nishita, M., Minami, Y., Yamaoka, A., Abe, T., Shigeta, M. and Morimoto, M. (2018). [Synchronized mesenchymal cell polarization and differentiation shape the formation of the murine trachea and esophagus](#). *Nat Commun* 9(1): 2816.
- Knot, H. J. and Nelson, M. T. (1998). [Regulation of arterial diameter and wall \[Ca<sup>2+</sup>\] in cerebral arteries of rat by membrane potential and intravascular pressure](#). *J Physiol* 508 ( Pt 1)(Pt 1): 199-209.
- Kwon, H. B., Wang, S., Helker, C. S., Rasouli, S. J., Maischein, H. M., Offermanns, S., Herzog, W. and Stainier, D. Y. (2016). [In vivo modulation of endothelial polarization by Apelin receptor signalling](#). *Nat Commun* 7: 11805.
- Landing, B. H. and Dixon, L. G. (1979). [Congenital malformations and genetic disorders of the respiratory tract \(larynx, trachea, bronchi, and lungs\)](#). *Am Rev Respir Dis* 120(1): 151-185.
- Li, Y. and Dudley, A. T. (2009). [Noncanonical frizzled signaling regulates cell polarity of growth plate chondrocytes](#). *Development* 136(7): 1083-1092.
- Lin, S. S., Tzeng, B. H., Lee, K. R., Smith, R. J., Campbell, K. P. and Chen, C. C. (2014). [Cav3.2 T-type calcium channel is required for the NFAT-dependent Sox9 expression in tracheal cartilage](#). *Proc Natl Acad Sci U S A* 111(19): E1990-1998.
- Muzumdar, M. D., Tasic, B., Miyamichi, K., Li, L. and Luo, L. (2007). [A global double-fluorescent Cre reporter mouse](#). *Genesis* 45(9): 593-605.
- Nobes, C. D. and Hall, A. (1999). [Rho GTPases control polarity, protrusion, and adhesion during cell movement](#). *J Cell Biol* 144(6): 1235-1244.
- Park, J., Zhang, J. J., Moro, A., Kushida, M., Wegner, M. and Kim, P. C. (2010). [Regulation of Sox9 by Sonic Hedgehog \(Shh\) is essential for patterning and formation of tracheal cartilage](#). *Dev Dyn* 239(2): 514-526.
- Sala, F. G., Del Moral, P. M., Tiozzo, C., Alam, D. A., Warburton, D., Grikscheit, T., Veltmaat, J. M. and Bellusci, S. (2011). [FGF10 controls the patterning of the tracheal cartilage rings via Shh](#). *Development* 138(2): 273-282.
- Schneider, C. A., Rasband, W. S. and Eliceiri, K. W. (2012). [NIH Image to ImageJ: 25 years of image analysis](#). *Nat Methods* 9(7): 671-675.
- Shyer, A. E., Tallinen, T., Nerurkar, N. L., Wei, Z., Gil, E. S., Kaplan, D. L., Tabin, C. J. and Mahadevan, L. (2013). [Villification: how the gut gets its villi](#). *Science* 342(6155): 212-218.
- Sinner, D. I., Carey, B., Zgherea, D., Kaufman, K. M., Leesman, L., Wood, R. E., Rutter, M. J., de Alarcon, A., Elluru, R. G., Harley, J. B., et al. (2019). [Complete Tracheal Ring Deformity. A Translational Genomics Approach to Pathogenesis](#). *Am J Respir Crit Care Med* 200(10): 1267-1281.

- Soeda, T., Deng, J. M., de Crombrughe, B., Behringer, R. R., Nakamura, T. and Akiyama, H. (2010). [Sox9-expressing precursors are the cellular origin of the cruciate ligament of the knee joint and the limb tendons.](#) *Genesis* 48(11): 635-644.
- Wirth, A., Benyo, Z., Lukasova, M., Leutgeb, B., Wetschureck, N., Gorbey, S., Orsy, P., Horvath, B., Maser-Gluth, C., Greiner, E., et al. (2008). [G12-G13-LARG-mediated signaling in vascular smooth muscle is required for salt-induced hypertension.](#) *Nat Med* 14(1): 64-68.
- Yin, W., Kim, H. T., Wang, S., Gunawan, F., Li, R., Buettner, C., Grohmann, B., Sengle, G., Sinner, D., Offermanns, S., et al. (2019). [Fibrillin-2 is a key mediator of smooth muscle extracellular matrix homeostasis during mouse tracheal tubulogenesis.](#) *Eur Respir J* 53(3). doi:10.1183/13993003.00840-2018
- Yin, W., Kim, H. T., Wang, S., Gunawan, F., Wang, L., Kishimoto, K., Zhong, H., Roman, D., Preussner, J., Guenther, S., et al. (2018). [The potassium channel KCNJ13 is essential for smooth muscle cytoskeletal organization during mouse tracheal tubulogenesis.](#) *Nat Commun* 9(1): 2815.

## Supplementary information

The following supporting information can be downloaded [here](#):

1. Supplementary Figure 1. Isolated embryos from euthanized animals
2. Supplementary Figure 2. Dissection of the trachea and lungs from the embryo
3. Supplementary Figure 3. Length and width measurements of the SM cell nucleus using the ImageJ software